

Dissociation of Vortex Stacks into Fractional-Flux Vortices

A. De Col^a, V. B. Geshkenbein^{a,b}, and G. Blatter^a^aTheoretische Physik, ETH-Honggerberg, CH-8093 Zurich, Switzerland and^bL.D. Landau Institute for Theoretical Physics RAS, 117940 Moscow, Russia

(Dated: April 14, 2024)

We discuss the zero field superconducting phase transition in a finite system of magnetically coupled superconducting layers. Transverse screening is modified by the presence of other layers resulting in topological excitations with fractional flux. Vortex stacks trapping a full flux and present at any finite temperature undergo a dissociation transition which corresponds to the depairing of fractional-flux vortices in individual layers. We propose an experiment with a bi-layer system allowing to identify the dissociation of bound vortex molecules.

The zero field superconducting to normal transition in thin films and layered superconductors is triggered by the proliferation of topological defects; the unbinding of Pearl vortices [1] in thin films and of pancake vortices [2] in layered superconductors generates a Berezinskii-Kosterlitz-Thouless transition (BKT) [3] which has been studied in detail [4, 5]. New features emerge when going to a system with a finite number N of magnetically coupled layers. Besides Pearl type vortex stacks penetrating through the full array of layers, cf. Fig. 1 (a), fractional-flux vortices appear which reside within the individual layers [6, 7], the analogue of the pancake vortices in a layered material; the reduced trapped flux associated with these vortices is due to the presence of other layers modifying transverse screening in the multi-layer system. The Pearl vortex can be viewed as a linear arrangement (stack) of fractional-flux vortices; the intra-layer unbinding transition of these fractional-flux vortices then corresponds to the dissociation of full-flux vortex stacks present at any temperature, cf. Fig. 1 (b). In this letter, we discuss the prospects of observing this dissociation transition in an experiment; in particular, we study a bi-layer system in a counterflow geometry which allows to observe the dissociation of vortex molecules into half-flux vortices, cf. Fig. 1 (c).

The basic prerequisite for the appearance of a BKT transition is the logarithmic interaction between defects, $V(R) = 2e^2 \ln R$, where we attribute an effective charge e to the defects. In the absence of screening, e.g., in a superfluid ^4He film, the logarithmic interaction between vortices extends to infinity and the system undergoes a finite temperature BKT transition [3]. In a superconducting film, transverse screening restricts the log-interaction to the screening length λ ; the Pearl vortices assume a finite self-energy $V(\lambda) = 2$ and hence can be thermally excited at any finite temperature | the superconducting to normal transition then is shifted to $T = 0$, although a sharp crossover survives at a finite temperature T_{BKT}^x $e^2 = 2$ [4]. Below, we concentrate on a system with N magnetically coupled superconducting layers, i.e., vortices interact through the transverse magnetic potential A , while the Josephson coupling due to Cooper pair tunneling between the layers is assumed to be negligible, as it is the case in a material with insu-

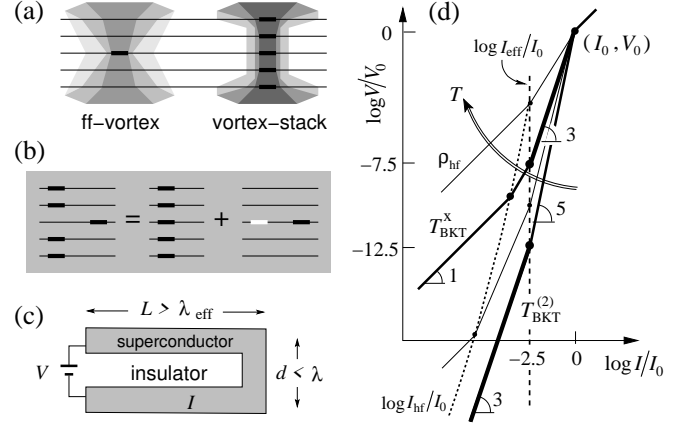


FIG. 1: (a) Fractional flux vortex and vortex stack in a $N = 5$ -layer system. (b) The excursion of one vortex from the vortex stack is equivalent to the combination of a complete stack and a vortex (anti-vortex pair; pair unbinding in a layer is equivalent to stack dissociation). (c) Geometry for the bi-layer setup shortcircuiting the effect of vortex stacks. (d) Sketch of I - V curves at various temperatures (see arrow); the algebraic dependence V/I with $\gamma > 3$ at low temperatures turns ohmic ($\gamma = 1$) at high temperatures. The regime between $T_{\text{BKT}}^{(2)}$ and T_{BKT}^x contains the interesting features associated with half-flux vortices. The current scale I_e ($I_0 = I_e$) (vertical dashed line) separates the physics of unscreened vortices from that of half-flux vortices. At $T_{\text{BKT}}^{(2)}$ the I - V curve exhibits the characteristic exponents 3 and 5 at small and large currents tracing the crossover from unscreened to half-flux vortices. Above $T_{\text{BKT}}^{(2)}$ an additional ohmic regime due to free half-flux vortices appears at low currents; the dotted line marks the crossover current I_{hf} . At temperatures $T > T_{\text{BKT}}^x$ the ohmic regime takes over and leaves only a small non-linear region at high currents probing unscreened vortices.

lating layers separating the superconducting ones. The presence of additional layers leads to drastic modifications in the potential $V(R)$ between individual vortices in the same layer: i) the log-interaction extends to infinity, ii) the magnetic flux Φ trapped by individual vortices is reduced to a fraction $1/N$ of the flux unit $\Phi_0 = hc/2e$, $\Phi(N) = \Phi_0/N$; the effective coupling e^2 in the interaction potential between defects is reduced correspondingly, $e^2 \rightarrow e^2/N$ [1–14]. Hence, the additional layers act

on the vortices in the same way as a dielectric matrix acts on charged particles. The unbinding of the fractional- $\Phi_0/2\pi$ vortices triggers a finite temperature BKT transition at $T_{\text{BKT}}^{(N)}$ [1–1+N]=2. At the same time, vortex stacks are present at any temperature; the unbinding of () vortices at $T_{\text{BKT}}^{(N)}$ then describes the dissociation of the vortex stacks rather than the superconductor-normal transition which, strictly speaking, appears already at $T = 0$. Finally, in a bulk layered superconductor, the magnetic field escapes in the transverse direction and the flux trapped by pancake vortices saturates at $\Phi_t = d_0/2$, where d and d_0 denote the layer separation and the bulk planar penetration depth. The pancake-vortex unbinding at $T_{\text{BKT}}^{(1)}$ [2]=2 describes a generic phase transition as no competing stacks show up in the bulk.

Below, we address the prospect of observing fractional- $\Phi_0/2\pi$ vortices in an experiment. The presence of vortices and their unpairing reveals itself in the current-voltage characteristic. Fractional- $\Phi_0/2\pi$ vortices appear most prominently in a bi-layer system, see Fig. 1(c). We propose a counterflow experiment where the contribution of stacks (vortex molecules) is eliminated. The current-induced unpairing of vortices then produces an algebraic characteristic V/I ; the change in the exponent from $\alpha = 3$ to 5 with increasing current, cf. Fig. 1(d), is a manifestation of the stack dissociation transition at $T_{\text{BKT}}^{(2)}$. In the following, we briefly derive the structure of topological excitations in layered systems, discuss their thermodynamics, and analyze the features in the I-V characteristic related to fractional- $\Phi_0/2\pi$ vortices.

Consider a superconductor of thickness d and with a London penetration depth λ . Central to our discussion is the interaction potential $V(R)$ between vortices: The current associated with a vortex is driven by the 2-phase twist $r' = \nabla_z R = R^2$, $j(R) = (c/4\pi^2)[r'_{\theta=2} + A(R)]$; transverse screening through the vector potential A reduces the action of r' until complete compensation is reached once a full flux quantum Φ_0 is trapped. A second vortex placed a distance R away is subject to the Lorentz force $F(R) = j(R)d_0/c = (2\Phi_0 d/R)[1 - (R) = \Phi_0]$, where $(R) = 2RA(R)$ is the flux accumulated within the distance R and $\Phi_0 = (\Phi_0/4\pi^2)^2$ is the line energy; integrating this force provides us with the desired potential between the vortices. The incomplete asymptotic screening with a reduced trapped flux $\Phi_t = (1 - (R))\Phi_0 < \Phi_0$ then gives rise to a logarithmic interaction $V(R) = 2\Phi_0 d [1 - (R)] \ln(R)$ and hence a BKT phase transition (note that $e^2 \propto \Phi_0 d$).

In order to find the flux Φ_t we have to solve the Maxwell equations for the potential A . We consider a stack of N superconducting layers of thickness d_s and separated by a distance d . The penetration depth λ_s of the layer material defines the bulk planar penetration depth $\lambda^2 = \lambda_s^2 d = d_s$. We place the vortex at the origin of the layer positioned at $z = 0$ and describe the protecting layers of thickness $d^< = (N - n)d$ and $d^> = (n - 1)d$

above and below the film in a continuum approximation. The system

$$\begin{aligned} r^2 A - \frac{1}{2} A &= \frac{d}{2} A + \frac{\Phi_0}{2} r' \quad (z); \quad d^< < z < d^>; \\ r^2 A &= 0; \quad z < d^< \text{ and } z > d^> \end{aligned} \quad (1)$$

then assumes the solution

$$A(R; z) = \frac{\Phi_0 d}{2} \int_0^z \frac{dK}{2} \frac{J_1(KR)}{C(K)} f(K; z); \quad (2)$$

with J_1 the Bessel function and the function $f(K; z) = [1 - d^0(K)]e^{K_+ z} + d^0(K)e^{K_- z}$ describing the z -dependence within the superconductor. Here, $d^0(K) = \frac{(K_+ - K_-)}{K^2 + \frac{1}{2}} = [(K_+ + K_-)e^{2K_+ d^0} + (K_+ - K_-)]$, with $K_+ = \frac{1}{2} \sqrt{K^2 + \frac{1}{2}}$ and $d^0 = d^< (d^0 = d^>)$ in the region $d^< < z < d^> (0 < z < d^>)$. The denominator $C(K)$ assumes the form $C(K) = [1 - 2d^<(K)]K_+ + [1 - 2d^>(K)]K_- + d^2$. Outside the superconductor, the field is obtained by replacing $z > 0 (z < 0)$ by $d^> (-d^<)$ in f and an additional correction factor $\exp[K(d^> - z)]$ ($\exp[K(d^< + z)]$). The Pearl- and pancake vortices are recovered in the limits $d^< ; d^> = 0$ and $d^< ; d^> = 1$.

The magnetic flux Φ_t trapped by a vortex is extracted from the vector potential at $z = 0$; for a thin N -layer system with $Nd \gg d_0$ we find the asymptotic form

$$A(R; z = 0) = (\Phi_t/2R)(1 - (R) = R) \quad (3)$$

with parameters $\Phi_t = 2\Phi_0 d/N$ and $(R) = \Phi_0/N$ independent of the layer position n . For large N the trapped flux saturates at the value $\Phi_t = d_0/2$ and $(R) = 0$ [8], while $\Phi_t = \Phi_0$ and $(R) = 2\Phi_0/d_s$ for the thin film. The decrease $\Phi_t = \Phi_0/N$ in trapped flux with increasing number of layers is easily understood: with $Nd \gg d_0$, the same magnetic field (and hence the same flux) is penetrating the N layers. On the other hand, a vortex stack (i.e., N () vortices) carries a full flux Φ_0 . The flux associated with one individual () vortex then is a fraction $1/N$ of the value trapped by the vortex stack and thus $\Phi_t = \Phi_0/N$.

The incomplete screening of the vortex singularity produces a log-interaction between vortices, $V(R) = 2\Phi_0 d \ln(R)$ at small distances $R \ll d_0$ and $V(R) = 2\Phi_0 d [\ln(d_0) + [1 - (R)] \ln(R/d_0)]$ involving a large self-energy but a reduced prefactor at large distances $R \gg d_0$. This logarithmic interaction competes with the entropy of vortex-pair excitations and triggers a Berezinskii-Kosterlitz-Thouless transition at [7, 11]

$$T_{\text{BKT}}^{(N)} = \frac{\Phi_0 d}{2} \left[1 - \frac{\Phi_t(N)}{\Phi_0} \right] \quad (4)$$

In a thin film, $\Phi_t = \Phi_0$ and the finite range of the interaction between Pearl vortices pushes the real transition to $T = 0$, in agreement with (4); the presence of one additional ‘protecting’ layer changes the situation: transverse screening reduces the trapped flux to half its value,

$t = t_0 = 2$, thus extending the range of the logarithmic interaction to infinity and pushing the transition temperature to a finite value $T_{BKT}^{(2)} = \mu_0 d = 4$. Adding more $(N - 1)$ layers, the trapped flux $t = t_0 = N$ decreases further until assuming the asymptotic value $t = d = 2$ in a bulk superconductor where $T_{BKT}^{(1)} = \mu_0 d = 2$ is largest.

The appearance of a finite temperature phase transition due to the protecting action of additional superconducting layers has its counterpart in multigap superconductors [12], cf. also Ref. 13. In both cases, the creation of a topological defect in one superconducting component or layer induces screening currents in the other components/layers via coupling to the common gauge field A ; the resulting incomplete screening extends the interaction between defects to infinity, although with a reduced 'charge'. A finite Josephson coupling between the layers or between the components of a multigap superconductor spoils this phenomenon through the appearance of a linear confining potential. While this coupling can be (made) arbitrarily small in a layered system, the internal Josephson effect in a multi-component superconductor cannot be tuned and is not necessarily small [14].

The setup where fractional-flux vortices make their most prominent appearance is the bi-layer system. Its thermodynamic properties are obtained from an extension of the renormalization group analysis in a $2D$ [9, 10] and involves the flow of the superfluid density $K(R)$ at scale R with $K(\ell) = K_0 = \mu_0 d = T$ and the vortex fugacity $y(R)$, with $(y=R)^2$ the density of vortex (anti-vortex) pairs of size R . Here, the renormalization involves a two-stage process: i) unscreened vortex pairs are integrated out on scales $R < \xi_e$ and provide renormalized values $(K; y)$ at $R = \xi_e$; ii) the flow is restarted with a reduced coupling $\mu_0 d = 2$ and half-flux (hf) vortex pairs are integrated out on scales $R > \xi_e$. We obtain the following results (see [15] for details): At temperatures $T < T_{BKT}^{(2)} = \mu_0 d = 4$ the initial fugacity $y_0 = \exp(-E_c/T)$ due to the core energy $E_c = \mu_0 d$ flows to zero and the superfluid density $K \rightarrow K_0 > 4$ remains finite. Above $T_{BKT}^{(2)}$ (hf) vortices start unbinding: a narrow critical regime (with a correlation length $\xi_{hf} = \xi_e \exp(-2/bt)$, $t = (T - T_{BKT}^{(2)})/T_{BKT}^{(2)}$ and b a dimensionless parameter) is followed by a mean-field behavior where the fugacity diverges to infinity and the renormalized superfluid density vanishes beyond the correlation length ξ_{hf} , defining a density of free (hf) vortices

$$n_{hf} = \frac{1}{2} \frac{y_0^{2=K}}{\xi_e} = \frac{2}{4} \frac{K}{\xi_e} = \frac{2}{4} \frac{P}{\xi_e} \frac{a}{t}; \quad (5)$$

with a of order unity. On approaching $T_{BKT}^x = \mu_0 d = 2$ the correlation length becomes comparable to ξ_e ; beyond T_{BKT}^x unscreened vortices start unbinding at small scales below ξ_e . Note that vortex stacks do preempt the superconducting transition of the bi-layer system but preserve superconductivity within the individual layers; indeed,

the force of a (hf) vortex acting on a vortex stack vanishes rapidly beyond the effective screening length ξ_e due to the complete screening of vortex stacks.

The presence of (hf) vortices can be traced in an experiment measuring the I-V characteristic (we denote the sheet-current density by $I = jd$). In the counterflow geometry of Fig. 1(c), the applied dc current acts oppositely on the two (hf) vortices constituting a stack and the linear response due to drag motion is quenched. The current-induced dissociation of pairs and stacks of (hf) vortices produces a non-linear I-V characteristic; the change in slope from 3 at low currents to 5 at high currents signals the thermodynamic dissociation of stacks at $T_{BKT}^{(2)}$. The current-induced unbinding of (hf) vortex pairs involves a thermal activation over the barrier $U(I) = \max_R [V(R) - I_0 R] = 2\mu_0 d \ln(R_I)$ at small distances $R_I \ll \xi_e$, while $U = 2\mu_0 d \ln(\xi_e) + \mu_0 d \ln(R_I = \xi_e)$ for $R_I \gg \xi_e$. Here, $R_I = I_0/I$ denotes the unbinding scale and $I_0 = 2\mu_0 dc = j_0$ is close to the depairing current. Applied currents smaller than $I_e = I_0 = j_0$ probe lengths larger than ξ_e and the effects of half-flux vortices become accessible.

The equilibrium density n_v of free vortices derives from the steady state solution of the rate equation [16] $\partial_t n_v = -n_v^2 =_{rec}$, with $\gamma = \exp(-U/T)$ the production rate of free vortices and $\gamma^2 =_{rec}$ the recombination parameter. Vortex drag then produces a finite non-linear resistivity, $\rho = \rho_n n_v$ with ρ_n the normal state resistivity, and a corresponding algebraic I-V characteristic $V = V_0 (I = I_0)^{(1)}$ with

$$(T; I) = 1 + K(T) [1 - t(R_I = \xi_e)]; \quad (6)$$

The exponent depends explicitly on the flux associated with the vortices: at short scales, unscreened vortices are probed and $\alpha = 1 + K$. On the other hand, large distances probe half-flux vortices and the exponent is reduced to $\alpha = 1 + K = 2$. The crossover between these two regimes appears at the current $I_e = I_0$. This reduction in α at I_e is the most prominent feature in the I-V characteristic signalling the presence of half-flux vortices in the system; at $T_{BKT}^{(2)}$, the change in slope is from 5 at large currents to 3 at low currents, cf. Fig. 1(d). The associated voltage signals are weak as the density of free vortices is already small, $n_v = 1/\xi_e^2$ at T_{BKT}^x and $n_v = 2/\xi_e^2$ at the true transition point $T_{BKT}^{(2)}$.

The temperature $T_{BKT}^{(2)}$ defines a resistive transition due to the proliferation of free half-flux vortices. Above $T_{BKT}^{(2)}$ the ohmic resistance appearing at low currents $I < I_{hf} = I_0 = j_0$ (probing distances larger than the correlation length ξ_{hf}) is determined by the density of free (hf) vortices, $\rho = \rho_n^2 n_{hf}$. In the mean-field regime above $T_{BKT}^{(2)}$ we can make use of (5) and find the location of the crossover at $I_{hf} = I_0(\xi_e) = (P/\xi_e)^{a=2t}$ and the temperature dependent resistivity $\rho_{hf}(T) = \rho_n(\xi_e)^2 (P/\xi_e)^{a=t}$ due to free half-flux vortices.

The measurement of I_{hf} or ρ_{hf} in this regime provides direct access to the correlation length ξ_{hf} and its mean-field like temperature dependence.

In order to analyze the BKT transition at $T_{BKT}^{(2)}$ various experimental constraints have to be accounted for: i) The system must be larger than the screening length ξ_e beyond which (hf) vortices appear. The relation (4) implies that $\xi_e(T_{BKT}^{(2)}) \approx 0.5 \text{ cm} = (T_{BKT}^{(2)} \text{ in K})$, hence $\xi_e \approx 1 \text{ mm}$ in a typical low T_c material. ii) Both the interlayer distance d and the layer thickness d_s have to be small compared to the bulk penetration depth λ . iii) The Josephson coupling has to be small enough to push the confinement length $\xi_c = (\bar{j}_0 = j_J) d$ beyond ξ_e ; separating the superconducting layers with an insulator [17] the Josephson current j_J can be made arbitrarily small. iv) The mean-field temperature dependence $\propto (1 - T^2/T_c^2)^{1/2}$ of the parameters and tends to push the temperatures $T_{BKT}^{(2)}$ and T_{BKT}^x towards the mean-field critical temperature T_c , $(T_{BKT}^x - T_{BKT}^{(2)}) = T_c$, $(T_c - T_{BKT}^x) = T_c - 4G\lambda^2 d^2$ with $G\lambda^2 d^2 = T_c = 2\lambda_0^2 (T = 0)d \approx 1$ the two-dimensional Ginzburg number [18]. A large Ginzburg number helps in distinguishing between the temperatures where (hf) and unscreened vortices unbind. v) The features in the I-V characteristic identifying the presence of (hf) vortices involve vortex densities which are suppressed by the small parameter $\epsilon = \xi_e$. Correcting parameters for the intrinsic dirtiness of thin films (see [19], we assume a mean free path limited by the layer thickness d_s) we obtain the estimates

$$[\epsilon = \lambda_{BKT}^{(2)}] \approx 1.5 \cdot 10^4 T_c^{1/2} d_s^{3/2} = \xi_{c0}; \quad (7)$$

$$G\lambda^2 d^2 \approx 3.2 \cdot 10^8 T_c^2 \xi_{c0}^2 = d_s^2; \quad (8)$$

where all lengths are measured in Å and temperatures in Kelvin. The results (7) and (8) tell us that given the (clean-) material parameters ξ_{c0} and ξ_{c0} it is not possible to maximize both $G\lambda^2 d^2$ and $\epsilon = \xi_e$ simultaneously by varying the thickness d_s . A reasonable compromise can be achieved if we choose a material with $\xi_{c0} \approx \xi_{c0}$ 1000 Å, $T_c \approx 10$ K, and a thickness $d_s \approx 500$ Å; this yields $\epsilon \approx 10^{2.5}$ and $G\lambda^2 d^2 \approx 10^4$. The small value of $\epsilon = \xi_e$ implies a small vortex density and requires a high voltage resolution, while the smallness of $G\lambda^2 d^2$ requires a temperature resolution in the mK range. The characteristic halving in ρ_{hf} signalling the presence of (hf) vortices below I_e involves voltages with $\log(V = V_0)$ between 7.5 and 12.5. With $V_{n,j_0 L} \approx 10$ mV (we assume $\xi_n \approx 100$ cm, $j_0(T_{BKT}^{(2)}) \approx 10^9 \text{ A/cm}^2$, and $L \approx 1$ cm) we find that an experimental voltage resolution in the sub-pico-Volt regime [20] allows to trace this halving in ρ_{hf} over a substantial temperature range below T_{BKT}^x , although the observation of this crossover at $T_{BKT}^{(2)}$ itself pushes the limits of present days experimental capabilities. Alternatively, one can trace the presence of (hf) vortices by measuring the characteristic mean-field type resistivity $\rho_{hf}(T)$ below T_{BKT}^x and through direct

observation with a scanning SQUID microscope [21].

An interesting analogy appears when comparing the present system with the bi-layer quantum Hall setup at total filling $\nu = 1$. The latter is expected to undergo a BKT transition into an interlayer phase coherent state, even in the absence of any tunneling between the layers [22]. The (hf) vortices discussed above (existing in one of two layers and with vorticity) correspond to topological excitations (merons) with charge $e=2$ and vorticity [23]; bound neutral meron pairs have their analogue in intralayer vortex (anti-vortex) pairs, while bound charged merons correspond to vortex stacks. The unbinding of meron-pairs in the BKT transition destroys the interlayer phase coherence and can be traced in the same type of counterflow experiment [24] as discussed above.

We acknowledge financial support from the Swiss National Science Foundation through the program MaNEP.

-
- [1] J. Pearl, Appl. Phys. Lett. 5, 65 (1964).
 - [2] J.R. Clem, Phys. Rev. B, 43, 7837 (1991).
 - [3] V.L. Berezinskii, Sov. Phys. JETP 32, 493 (1971); J.M. Kosterlitz and D.J. Thouless, J. Phys. C 6, 1181 (1973).
 - [4] A.M. Kadin, K. Epstein, and A.M. Goldman, Phys. Rev. B 27, 6691 (1983); A.T. Fiory, A.F. Hebard, and W.J. Glaberson, Phys. Rev. B, 28, 5075 (1983).
 - [5] S.N. Artemenko, I.G. Orlova, and Yu.I. Latyshev, JETP Lett. 49, 654 (1989); S. Martin et al., Phys. Rev. Lett. 62, 677 (1989).
 - [6] R.G. Mints, V.G. Kogan, and J.R. Clem, Phys. Rev. B, 61, 1623 (2000).
 - [7] V. Pudikov, Physica C 212, 155 (1993).
 - [8] In the bulk, corrections to the leading term $A \propto \xi_e^{-2} R$ are exponentially small for $R \gg \xi_e$.
 - [9] J.M. Kosterlitz, J. Phys. C 7, 1046 (1974).
 - [10] B. Horowitz, Phys. Rev. B 47, 5947 (1993).
 - [11] We use the properly renormalized line energy μ_0 , cf. J.V. Jose et al., Phys. Rev. B 16, 1217 (1977).
 - [12] E. Babaev, Phys. Rev. Lett. 89, 067001 (2002); E. Babaev, Nucl. Phys. B 686, 397 (2004).
 - [13] S. Sachdev, Phys. Rev. B 45, 389 (1992); J.P. Rodriguez, Phys. Rev. B 49, 9831 (1994); J. Smiseth, E. Smøgrav, A. Sudbo, Phys. Rev. Lett. 93, 077002 (2004).
 - [14] D.A. Gorokhov, cond-mat/0502083
 - [15] A. De Col, V.B. Geshkenbein, and G. Blatter, unpublished.
 - [16] B.I. Halperin and D.R. Nelson, J. Low Temp. Phys. 36, 599 (1979).
 - [17] With an exponential dependence on d , an insulator of a few nm thickness is sufficient.
 - [18] G. Blatter et al., Rev. Mod. Phys. 66, 1125 (1994).
 - [19] P.G. de Gennes, Superconductivity of Metals and Alloys (Addison-Wesley, New York, 1966).
 - [20] P.L. Gamma, L.F. Schneemeyer, and D.J. Bishop, Phys. Rev. Lett. 66, 953 (1991).
 - [21] F. Tafiri et al., Phys. Rev. Lett. 92, 157006 (2004).
 - [22] X.G. Wen and A. Zee, Phys. Rev. Lett. 69, 1811 (1992).
 - [23] K. Moon et al., Phys. Rev. B 51, 5138 (1995).
 - [24] M. Kellogg et al., Phys. Rev. Lett. 93, 036801 (2004).